



OPEN

## Efficient crystallization and extraction of lithium carbonate based on hair

Yang Zhang<sup>1</sup>, Yu-Han Huang<sup>1</sup>, Hou-Jie Wang<sup>1</sup>, Lin-Guo Zheng<sup>1</sup>, Qi-Yu Yang<sup>1</sup>, Yan-Ru Wang<sup>1</sup>, Jiang Zhao<sup>2</sup> & Cheng-Lu Jiang<sup>1</sup>✉

This study primarily focuses on utilizing hair strands to achieve the crystallization of lithium carbonate, aiming to investigate the factors influencing crystal formation and volume variation by altering external conditions. To research the reason of crystallization, we have identified the following influencing factors: the direction of crystal growth, the temperature, the evaporation rate, selection of containers. The study ultimately revealed that the container material, solution temperature, evaporation rate, and crystal growth surface all influence crystallization and crystal volume.

**Keywords** Lithium carbonate, Evaporation rate, Crystal, Dried hair, Temperature, Containers

Lithium (Li) has been hailed as one of the “important energy elements that drive the progress of the world” in the 21st century<sup>1</sup>. High-purity  $\text{Li}_2\text{CO}_3$  is widely used and is the main raw material for the preparation<sup>2</sup> of other high-purity lithium salt compounds<sup>3,4</sup>, lithium alloys and cutting-edge optoelectronic products.

Due to the increasingly prominent problem of environmental pollution<sup>10–12</sup>, people have begun to look for new energy storage methods, among which lithium battery energy storage has the characteristics of good cycle characteristics, fast response speed, and high system comprehensive efficiency, and is the most widely used energy storage method in the market<sup>5</sup>. Energy storage technology has become a leading force in promoting the world's energy development and transformation because it can provide an effective energy balance and energy storage for new energy sources. Lithium-ion batteries have the advantages of high specific energy, green and pollution-free<sup>6</sup>; In the face of the huge demand for energy storage development brought about by supporting the construction of new power systems<sup>7</sup> and ensuring how to promote lithium battery energy storage under the existing technical level, industrial base, and policy conditions<sup>8,9</sup>. The healthy and rapid development of the industry is an urgent problem facing the energy and power industry. Lithium carbonate is extracted from mineral resources<sup>10–12</sup> and its reserves in nature are very limited, with strong regionality and scarcity, and it is a scarce resource.  $\text{Li}_2\text{CO}_3$  is a stable and common lithium-based compound, which is widely used in batteries, glass, ceramics, pharmaceuticals and other industries, as well as portable electronic devices such as mobile phones and notebooks<sup>13</sup> and with the rapid development of the lithium battery industry and the development needs of other industries, the demand for lithium carbonate has surged in recent years.

The raw material of crystalline grade lithium carbonate prepared in the laboratory is lithium carbonate powder with a high concentration, and then the powder is subjected to crystallization experiments. Wang et al.<sup>14</sup> studied the effects of feeding rate, seed dosage, reaction temperature and stirring rate on lithium carbonate particle size by designing an L9(34) orthogonal table. Tao et al.<sup>11</sup> and Zhang et al.<sup>15</sup> studied the preparation process of lithium carbonate powder through single factor experiments. Duan et al.<sup>16</sup> optimized the reaction crystallization process of lithium carbonate by response surface method. In solid-state lithium batteries<sup>17</sup>, solid-state electrolyte is in rigid contact with the electrode particles, which is more sensitive to the volume change of the electrode material, and it is easy to cause the contact between the electrode particles and between the electrode particles and the electrolyte to deteriorate, or the stress accumulation causes the failure of the mechanical properties of the electrolyte, which in turn leads to the attenuation of the electrochemical performance of the battery. Repeated expansion and contraction lead to instability of the interface contact, and phenomena such as deformation, pulverization, and detachment between the current collector and electrode particles will occur, resulting in capacity decay. Therefore, good interfacial mechanical stability is also the key to obtaining high-performance solid-state batteries, but so far, there are few studies of this kind in solid-state batteries<sup>18</sup>, volume of the solid of the cathode material is not large enough, the utilization efficiency is still low, and the battery capacity is small.

<sup>1</sup>College of Water Conservancy and Hydropower Engineering, Sichuan Agricultural University, Ya'an 625014, People's Republic of China. <sup>2</sup>Ya Hua Lithium (Yaan) Co., LTD, Ya'an, Sichuan 625000, People's Republic of China. ✉email: juul@sicau.edu.cn

Xie et al.<sup>19</sup> used a laser particle size analyzer to detect the particle size of lithium carbonate, and the maximum particle size obtained was only 10  $\mu\text{m}$ <sup>19</sup>. Therefore, this study can use the experimental method to change the volume of the crystal.

Recent studies reveal that twisted porous fibers with an intrinsic hydrophilic core and hydrophobic surface enable spontaneous liquid transport through capillary action<sup>20</sup>. Upon immersing one end in a salt solution, water ascends the fiber, and subsequent evaporation drives solute supersaturation, resulting in crystallization.

By leveraging the hydrophilic and hydrophobic properties of fibers, we employed hair strands as crystallization substrates. As a renewable, eco-friendly, green, and low-cost material, using hair to facilitate lithium carbonate crystallization is undoubtedly highly innovative. Moreover, if adjusting external factors can induce controllable changes in crystal volume, it would mitigate adverse effects such as particle fragmentation and separation caused by small dimensions, as well as reduce issues like expansion and contraction under external forces. Consequently, the stability, utilization efficiency, and electrochemical performance of lithium carbonate crystals are enhanced, which is of great research significance for the future battery industry<sup>21</sup>.

## Experimental section

### Chemicals

Industrial distilled water was purchased from Zhejiang Nandai Industrial Co., Ltd.

Lithium carbonate powder  $\text{Li}_2\text{CO}_3$  ( $\geq 99.5\%$ ) from Shanghai Aladdin Biochemical Technology Co., Ltd.) and Sangon Biotech (Shanghai) Co., Ltd.

Dried hair strands (15–20 cm).

### Equipment

This paper, we use the Borosilicate glass(GG-17)beakers, conical flask(GG-17), Austenitic Stainless Steel(304) beakers, Polypropylene(PP)plastic beakers, glass test tubes(GG-17), hair strands, glass rods, Borosilicate glass slides, hot melt adhesive (for holding two glass slides), XRD(Rigaku Corporation D/max-RB) Instruments, Electron microscopy (COXEM)EM-30 N, Vacuum dry box, Plastic wrap, Rubber bands constant-temperature chamber. The sample was placed in the constant-temperature chamber for experimental observation.

### Preparation of lithium carbonate crystals

As shown in Fig. 1 lithium carbonate powder (1.55 g) is dissolved in 100 mL of distilled water at room temperature (22 °C) and stirred thoroughly. Once established, lithium carbonate powder exhibits limited solubility in water, with its solubility decreasing with increasing temperature. Therefore, the solution was placed in a low-temperature (0–5 °C) constant-temperature chamber with continuous stirring for approximately 20–30 min to maximize the dissolution of lithium carbonate powder in water. Then the solution was taken out and placed outdoors at a temperature of 20–25 °C and a humidity of 45%–65%. We selected dry hair from the same person, approximately 15 cm to 20 cm in length (ensuring it extends above the beaker). Then tape the dry hair to the glass sheet, submerging 2/3 of the hair in the solution. Hair strands were selected as crystallization substrates due to their extremely fine diameter, exceptional flexibility that facilitates bending, and strong water-absorption capacity. Composed of keratin, hair forms fiber bundles where these fibrils are tightly interconnected,

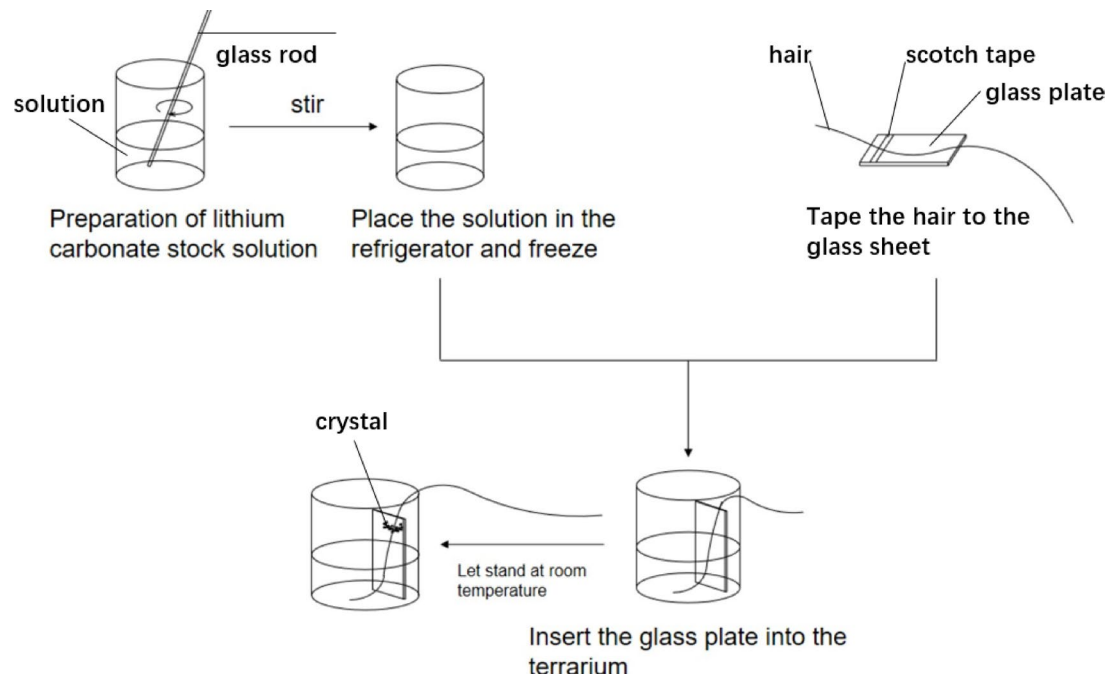


**Fig. 1.** Preparation of flowcharts.

constituting the main structure of hair - a characteristic remarkably similar to synthetic fibers. These unique properties make hair particularly effective in promoting lithium-ion adsorption from solution when immersed. If left for a day, crystals can be seen to precipitate around the hair, and over time, the crystals will appear in a large area around the hair, and after a few months of natural evaporation, crystals will appear at the bottom of the container and the walls of the cup<sup>22</sup>.

## Results and discussions

### Hair crystallization effect

There are two ways to place strands of hair; As shown in Fig. 2a,b, one is to suspend it in the solution without contact with the surface of any container. Another one is to keep the hair strands against the walls of the container; The test results showed that the hair strands attached to the walls of the container had crystals, while the hanging strands of hair did not show any symptoms. Through many experiments, it was observed that crystals crystallize around the hair strands, but they always start to crystallize in the hair strands at a certain height above the liquid level, rather than directly from the liquid surface. The crystals grew by the hair are snowflake-like<sup>23</sup> with a regular shape and a large area<sup>14</sup>. According to the electron microscope diagram in Fig. 3, the diameter of a crystal prepared in the laboratory can be accurately measured to be between 500  $\mu\text{m}$  ~ 1000  $\mu\text{m}$ ; The diameter of the sample powder is only 10  $\mu\text{m}$  ~ 15  $\mu\text{m}$ ; Obviously, the volume change from powder to crystal is 50 ~ 100 times.

### Selection of containers

As shown in Fig. 4, there are three cups, which are respectively stainless steel beaker, glass beaker and plastic beaker. Based on the above experiments, the experiments were conducted in such a way that the hair strands adhered tightly to the walls of the glass. In this experiment, borosilicate glass containing silicon dioxide ( $\text{SiO}_2$ ) and boron oxide ( $\text{B}_2\text{O}_3$ ) was used, with common types such as GG-17 (Schott Glass) beaker, the austenitic stainless steel (304) beaker and polypropylene (PP) plastic beaker. The experimental phenomena showed that the crystal grew by the borosilicate glass beakers were the largest and had more mass, and the shape was similar to snowflakes, followed by polypropylene (PP) plastic beakers, but the crystal shape was irregular and similar to cotton, and the austenitic stainless steel (304) beaker did not produce any crystals and did not have any phenomenon.

The main reason for the above phenomenon is that Schott glass contains oxygen elements, which provide excellent water absorption, thereby enabling the induction of crystal growth through the hair. Similarly, in polypropylene plastic beakers, the presence of polymer compounds also allows for water absorption, but due to the lower oxygen content, the shape and effect of crystal growth are far less pronounced than in Schott glass. Finally, in austenitic stainless-steel beakers, the presence of various metal elements (e.g., nickel, manganese) creates a repulsive effect that inhibits water absorption, preventing the hair from inducing crystallization in the solution. Thus, for the follow-up crystallization experiments, Schott glass beakers were selected due to their superior performance.

### Influence of the evaporation rate

The difference in the rate of nucleation and growth of the crystals directly affects the final crystal morphology. If the rate of nucleation of the crystal is greater than the growth rate of the crystal, more fine crystals will be produced, and eventually the agglomeration of crystal may occur, and vice versa, larger crystals may be produced. Through the control test shown in Fig. 5, a cup of prepared solution I (1.55 g/100mL) was put into a vacuum dry box to keep it in a vacuum environment; Another cup of the same solution II (1.55 g/100 mL) is placed outdoors (24 °C ~ 26 °C); The results show that at the temperature of 24 °C ~ 26 °C, the humidity is 45%~50%, and after 24 h, a small number of crystals appear on the glass plate of solution I. Under the outdoor condition, the hair precipitates crystals with a larger volume and a large mass.

The observed crystallization under vacuum conditions primarily results from compromised sealing integrity of the vacuum pump (The pressure reading of the vacuum pressure gauge changes). When the system remains

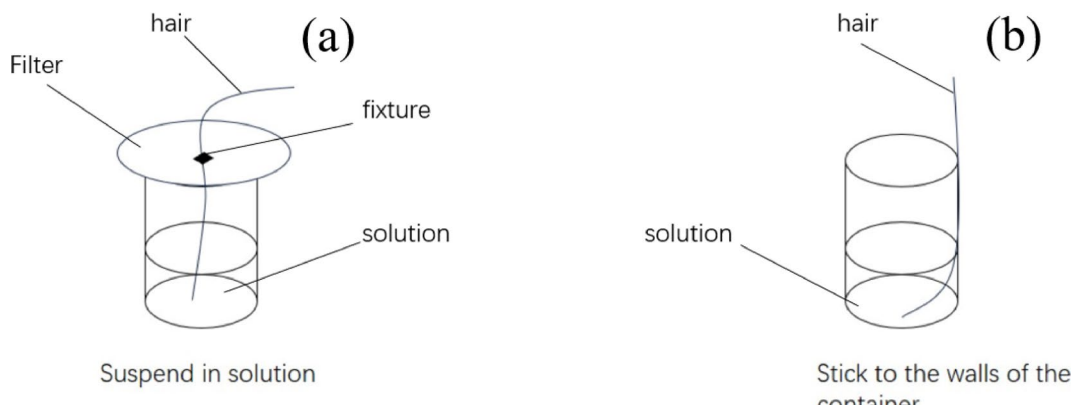


**Fig. 2.** Aerial and adherent specifications.

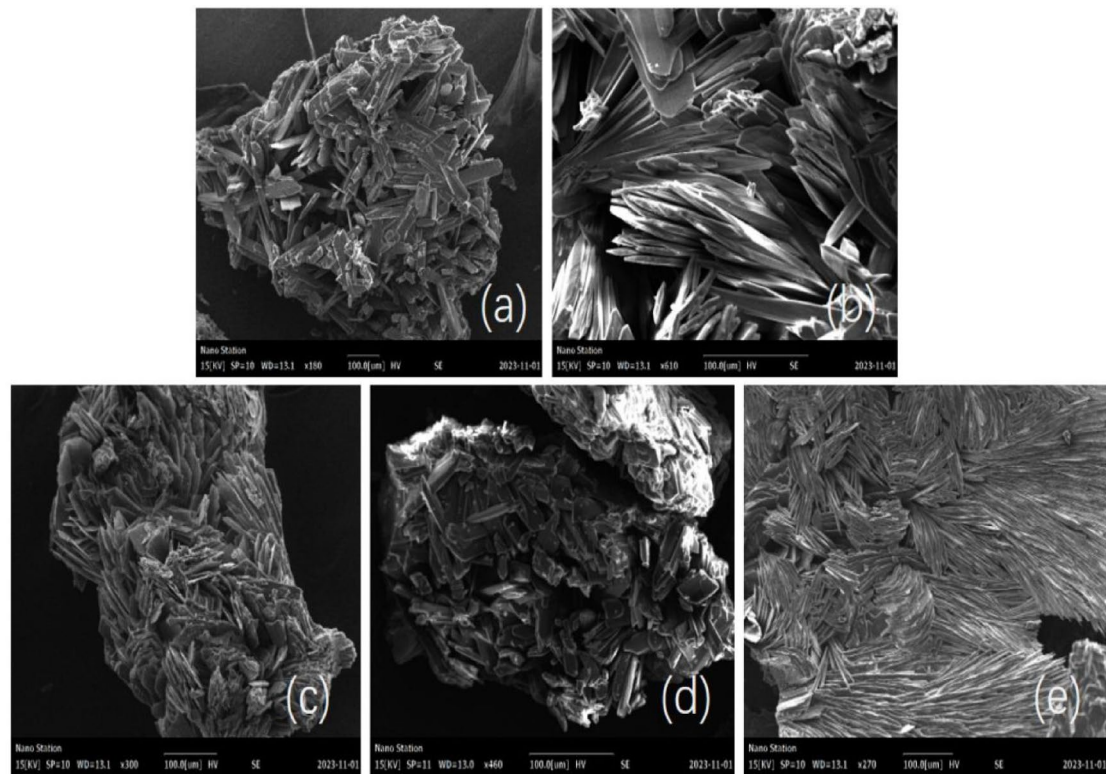


**Fig. 3.** The electron microscope image of the obtained crystal was prepared in this method. Voltage: 15kv; Magnification (a) 150/ (b) 610/ (c) 300/ (d) 460/ (e) 270.

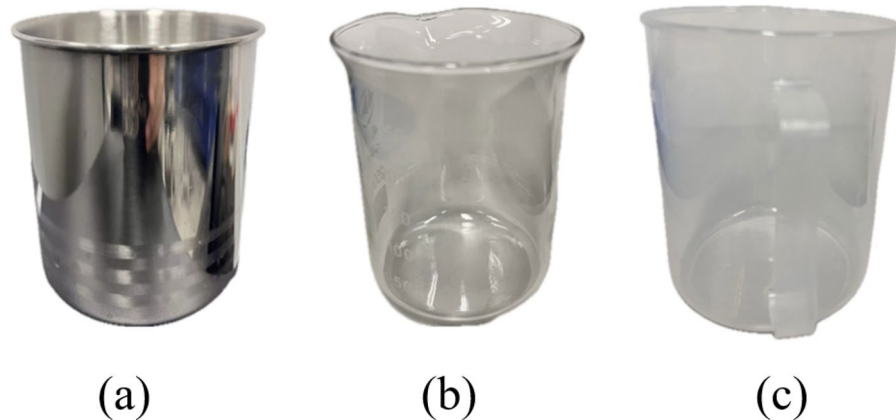


**Fig. 4.** (a) Stainless steel beaker (b) glass beaker (c) plastic beaker.

undisturbed for prolonged periods, this imperfect sealing allows gradual ingress of ambient air into the vacuum chamber. The subsequent minute air infiltration induces progressive solvent evaporation from the solution, ultimately triggering crystalline nucleation and growth.

The study reveals that crystal formation is drastically reduced in a vacuum (near-zero evaporation rate) compared to open-air conditions, confirming evaporation as the primary driver of crystallization. However, the minimal crystallization observed in a vacuum indicates that hair fibers can also induce nucleation. Overall, evaporation rate governs both the speed of crystallization and the ultimate crystal size. So, an experiment was conducted controlling the rate of evaporation around the hair.

As shown in Fig. 6, by providing the same temperature (14°C~17°C), coating the surface of the glass beaker with a film, and then creating holes in the film, different evaporation rates can be achieved by creating the same number of holes but with different pore sizes. The experimental procedure was as follows:

First, prepare a lithium carbonate solution with a concentration of 1.2 g/100mL. Then, place a strand of hair tightly against the inner wall of the beaker. Cover the entire mouth of the beaker with plastic wrap and

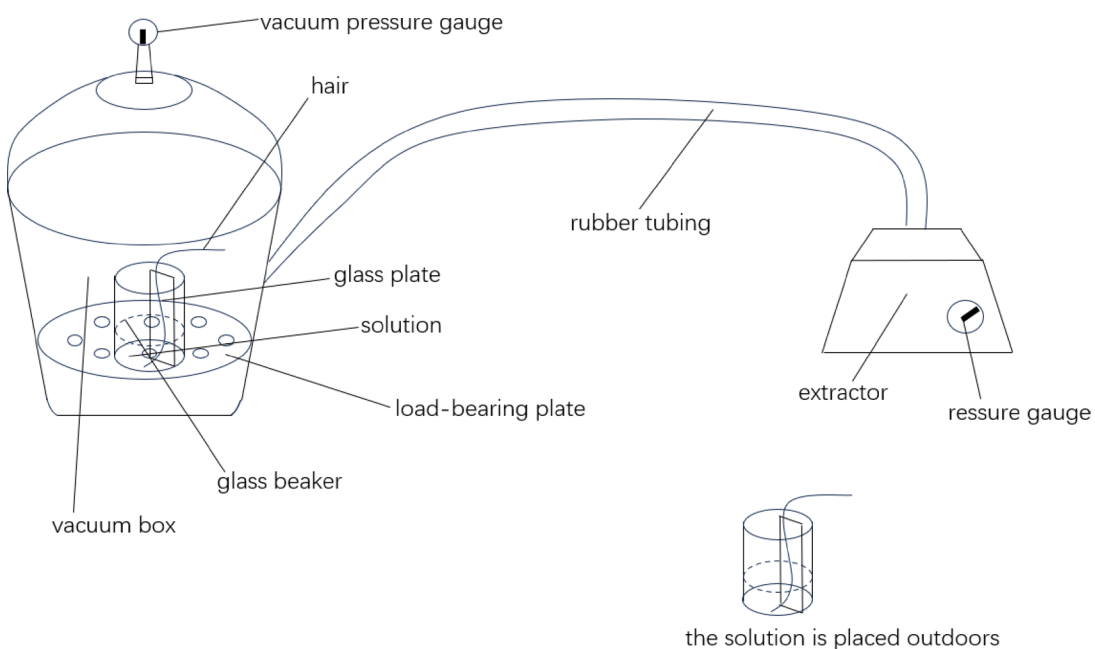


**Fig. 5.** Vacuum dry box.

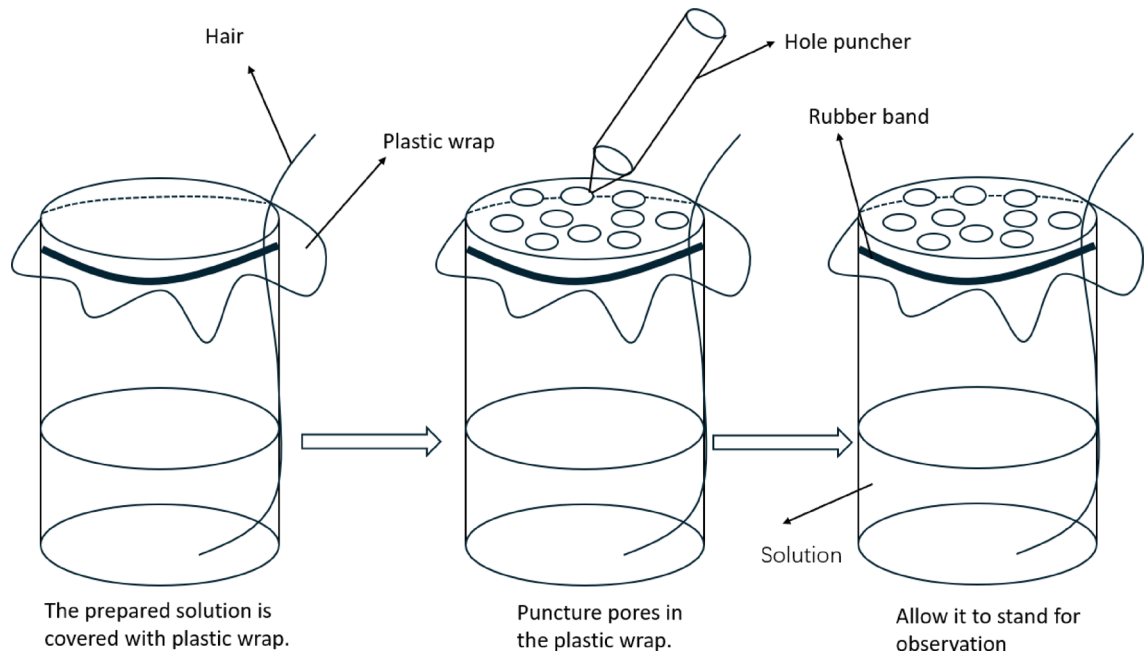


**Fig. 6.** Procedure for film coating and pore puncturing.

Pore size/mm	Crystal size/ $\mu\text{m}$ (red circle)
3.96 mm	23.3 $\mu\text{m}$
2.03 mm	75.0 $\mu\text{m}$
0.5 mm	192.8 $\mu\text{m}$

**Table 1.** Pore size and crystal size.

secure it tightly with a rubber band. Next, puncture pores in the plastic wrap with three different pore sizes: small (0.5 mm), medium (2.03 mm), and large (3.96 mm), with 10 holes for each size. Allow the setup to stand undisturbed for observation over a period of one month.

The following images are SEM (Scanning Electron Microscope) micrographs of the pores, ordered sequentially as: large pore, medium pore and small pore. The area enclosed by the red circle represents a relatively intact single crystal. Based on the magnification scale bar in the electron microscopy figure, the size of an individual complete crystal was calculated.

From the Table 1, it can be clearly observed that the crystal size formed in the small pore (192.8  $\mu\text{m}$ ) from Fig. 7. is significantly larger than that in the medium pore (75.0  $\mu\text{m}$ ) from Fig. 8. and large pore (23.3  $\mu\text{m}$ ) from Fig. 9. This further confirms the influence of evaporation rate on crystallization efficiency—a lower evaporation rate promotes larger crystal formation. From Fig. 10 (The red-circled area indicates the quantity of crystals) the experimental results demonstrate that while the small pore samples yield the largest crystal size, their production quantity is the lowest—significantly less than that of the medium pore. This phenomenon occurs because medium pore sizes accelerate the evaporation rate, thereby promoting faster crystal formation. However, excessively rapid crystallization kinetics ultimately limits the growth of individual crystal domains.

In the large-pore group, the plate-like crystals displayed rougher edges. This is attributed to excessively rapid crystallization, which induced internal stress that disrupted crystal growth, ultimately leading to smaller crystal dimensions compared to the small pore groups.

Therefore, the evaporation rate significantly influences crystallization outcomes. Lower evaporation accelerates crystal nucleation and growth, but excessively rapid evaporation can introduce internal stresses, leading to crystal defects and reduced crystal quality. Hence, controlling the evaporation rate is essential for optimal crystallization.

To further investigate this relationship, introduce temperature as a key variable to explore its correlation with crystal morphology, size, and structural integrity.

### Influence of temperature

First, a lithium carbonate solution of 1.8 g/150mL was prepared in a conical flask made of Schott glass. Then, five test tubes were prepared with a lithium carbonate solution of 0.12 g/10mL. After that, the hair was pressed firmly against the inner wall of the conical flask and test tube, making sure that two-thirds of the hair was immersed in the solution. Calculate the freezing point of the solution using the freezing point depression formula.

FORMULA:

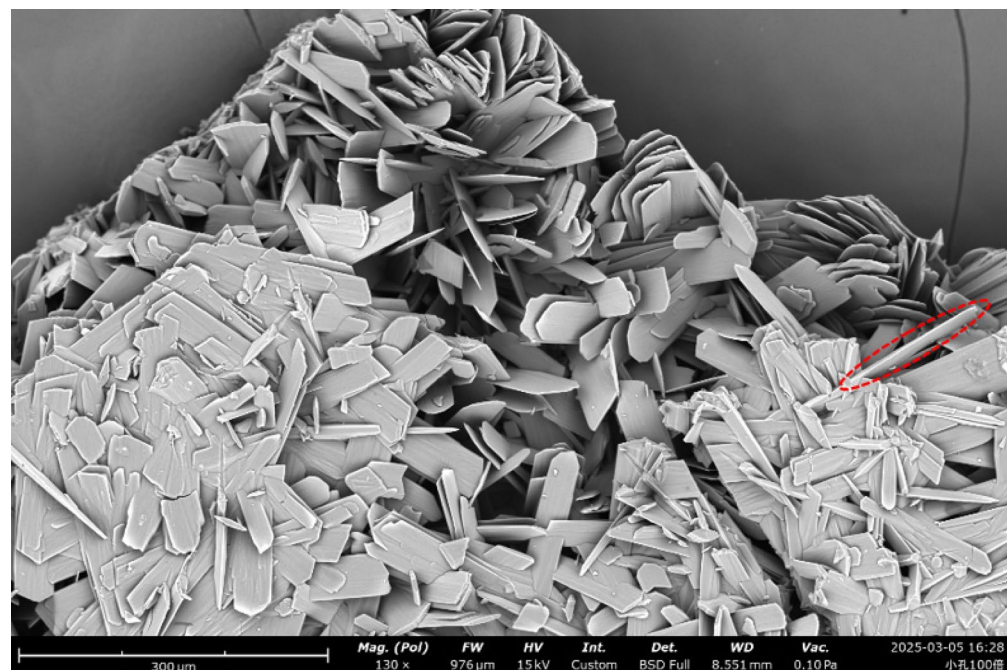
$$\Delta T_f = i \cdot K_f \cdot m \approx -0.785^\circ C$$

$\Delta T_f$ : The freezing point depression.

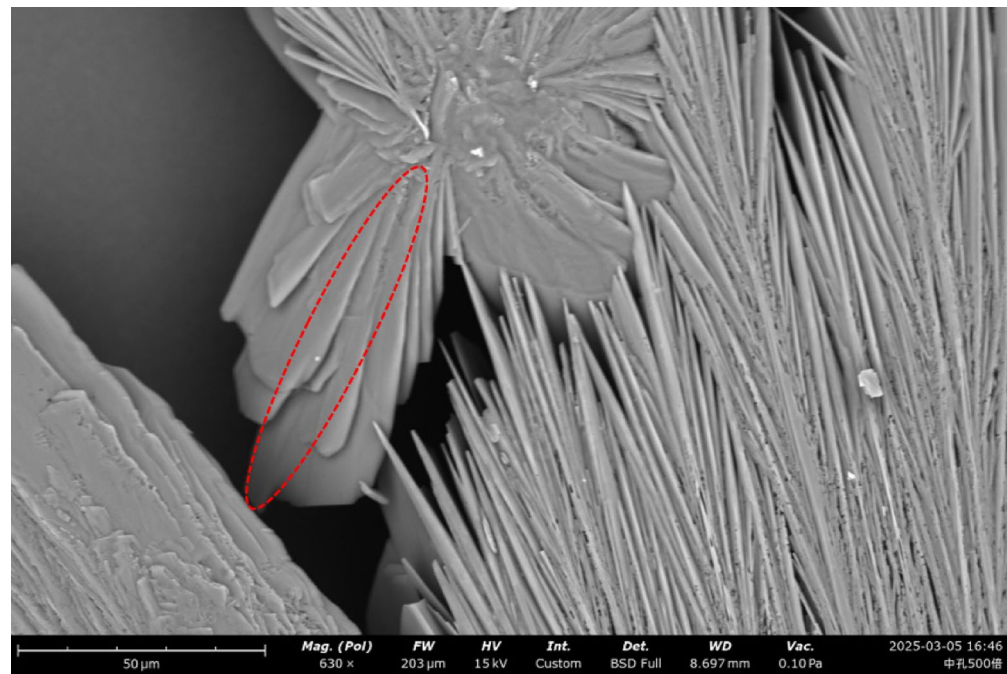
i: The van't Hoff factor (for  $\text{Li}_2\text{CO}_3$ ,  $i \approx 2.6$ ).

$K_f$ : The freezing point depression constant of water.

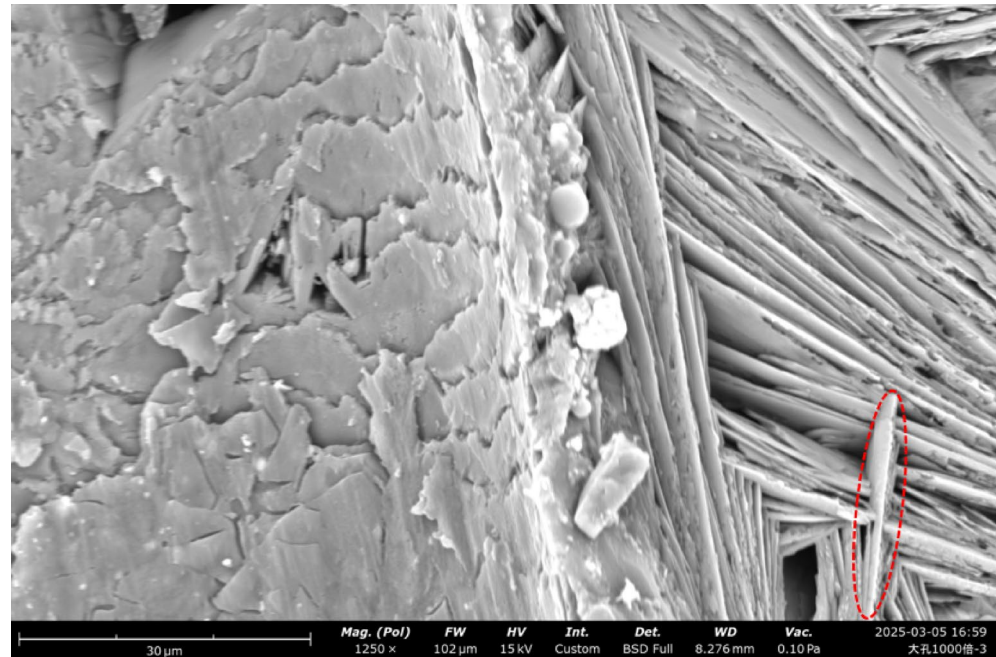
m: Molality(mol/kg).



**Fig. 7.** Small pore : The crystal size of the small pore is the largest, so only a 100 $\times$  magnification is needed to observe a complete crystal.

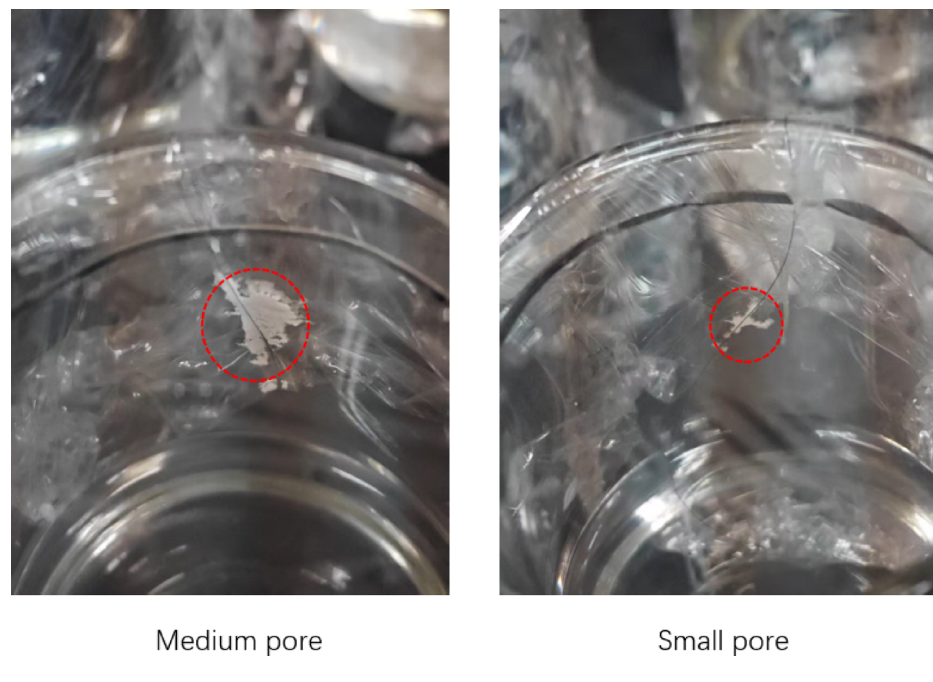
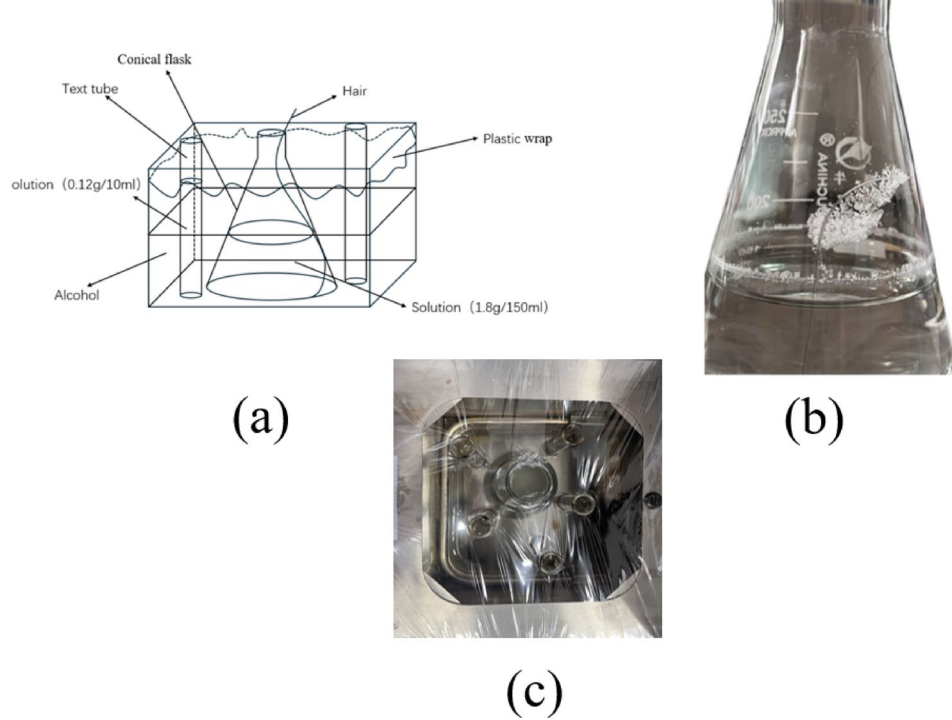


**Fig. 8.** Medium pore : The crystal size of the medium pore is slightly larger, so a magnification of 500× is sufficient to observe a relatively complete crystal.



**Fig. 9.** Large pore: The crystal size of the large pore is relatively small, it needs to be magnified with a magnification of 1000× to observe a relatively complete crystal.

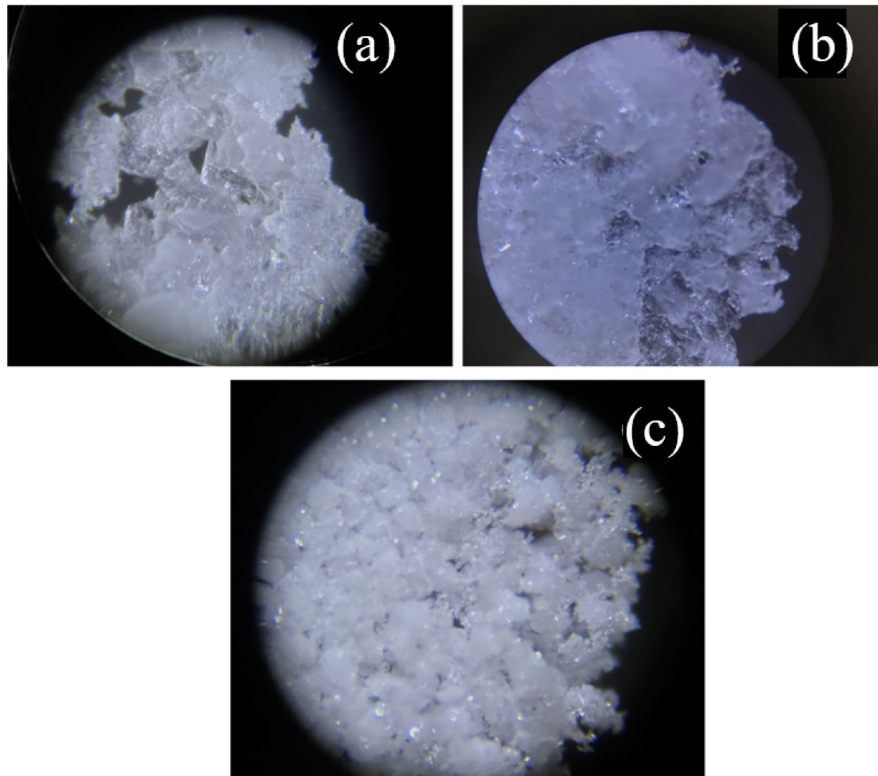
In this experiment, the temperature was controlled using a water bath variable temperature method. Since water freezes below 0 °C, alcohol was used instead of water in this experiment. As shown in Fig. 11(a), the conical flask and test tubes were placed in a constant-temperature chamber filled with alcohol (note that the height of the conical flask and test tubes should be greater than that of the chamber). Meanwhile, the hair strand should be entirely inside the container to prevent environmental disturbances (e.g.: air currents) from causing movement that could interfere with the results. The opening of the chamber was then covered with plastic wrap, and the portion covering the mouths of the conical flask and test tubes were cut away (to prevent

**Fig. 10.** Production quantity.**Fig. 11.** The conical flask is placed inside an incubator.

alcohol evaporation while allowing the solution to evaporate). The temperature was adjusted to study the effect of temperature on crystallization.

As shown in Table 2, the study found that crystallization was completely suppressed upon freezing of the solution. The optimal growth temperature for the crystals is between 0 °C and 10 °C. Within this range, it can be clearly observed from Fig. 11b that the crystal growth rate is slow, and the resulting crystals are relatively large. When the temperature exceeds 10 °C, the crystals grow faster but their size becomes smaller. The appearance of crystals formed at different temperatures under an electron microscope is shown in Fig. 12.

Temperature/°C	Experimental phenomena
-10°C~7.5°C	The solution freezes without crystallization.
-1°C~2.5°C	The bottom of the solution froze while the rest remained unfrozen, with no crystals forming.
4.5°C~8°C	Crystals precipitated out
8°C~14°C	The crystal continues to grow.

**Table 2.** Temperature and experimental phenomena.**Fig. 12.** (a) 0°C~10°C (b) 10°C~14°C (c)  $\text{Li}_2\text{CO}_3$  powder (The microscope has a 4x magnification).

The reason is that at lower temperatures, with less evaporation, lithium ions in the solution have sufficient time to aggregate, allowing the formation of larger single crystals. Conversely, at higher temperatures, under the same evaporation conditions, lithium ions crystallize more rapidly, leading to faster nucleation and resulting in smaller individual crystals.

Meanwhile, in the crystallization observed in the test tube, it has drawn the following conclusion: the length of hair strand closely adhering to the wall of the tube is denoted as  $L(\text{cm})$ . The red part in Fig. 13 is the length of  $L$ .

The longer  $L$  is, the greater the amount of crystallization. The reason lies in the fact that the hair strand requires a carrier to induce crystallization in the solution, meaning it must adhere closely to the wall. A shorter  $L$  indicates that a significant portion of the hair strand beneath the liquid surface is suspended in the solution. This portion of the hair strand does not contribute to crystal formation. Therefore, the actual length of the hair filament participating in crystallization is shorter, naturally resulting in less crystal formation.

**Shape of the crystalline area of the hair (Curved surface, vertical faces and horizontal faces)**  
 Experimental observation shows that both flat and curved surfaces<sup>16</sup> can produce large crystals with a regular shape in the shape of snowflakes. Experiments have shown that crystals grow around the hair strands, both vertically and horizontally. However, under the same temperature condition, the difficulty of growing crystals on the horizontal plane shown in Fig. 14a is far greater than that on the vertical planes shown in Fig. 14b,c. So, the crystalline plane has a certain influence on lithium carbonate crystallization.

The reason is that when the hair strand induces solution crystallization, the vertical and curved surfaces experience friction from the contact interface, which partially counteracts gravity. This prevents the crystals from easily detaching, allowing them to gradually accumulate over time. In contrast, on a horizontal surface, the absence of friction means the crystals must overcome gravity entirely, making it difficult for them to grow.

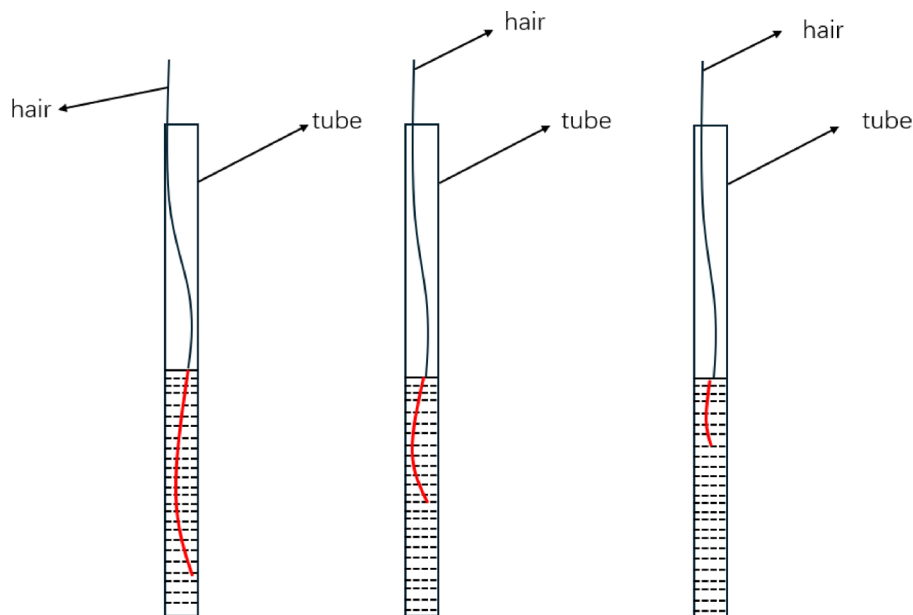


**Fig. 13.** The front view of the tubes.

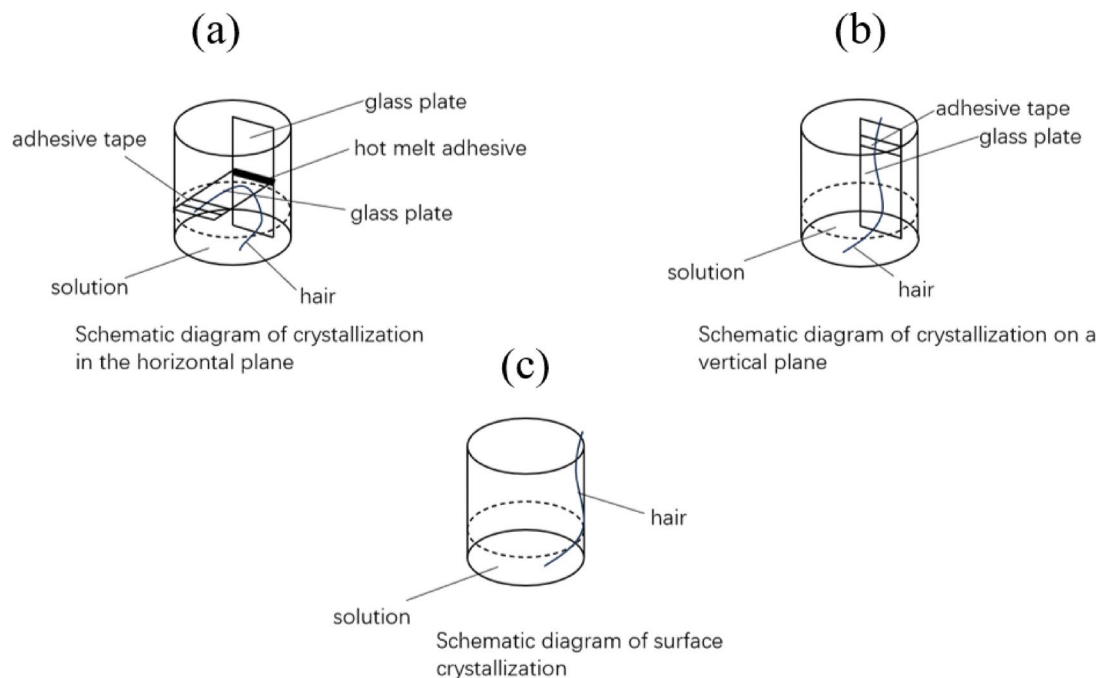


**Fig. 14.** Schematic diagrams of crystallization.

Another reason is that although placed under the same temperature conditions, the hair strands on the horizontal surface, because they are covered by a glass plate, have reduced contact with the air to some extent. Therefore, compared to the curved and vertical surfaces, which are directly exposed to the air above, the temperature of the hair strands on the horizontal surface is slightly lower than that of the curved and vertical surfaces. This further leads to the conclusion that the vapor pressure of water on the horizontal hair strands is lower than that on the curved and vertical surfaces. As a result, the evaporation of the horizontal hair strands is slower, leading to the formation of fewer crystals.

#### Product features

X-ray diffraction<sup>24,25</sup> analysis is used to characterize the crystalline morphology of the product. The diffraction peaks diffuse and most of the energy is absorbed by the samples using the copper  $\text{K}\alpha$  radiation test equipment.

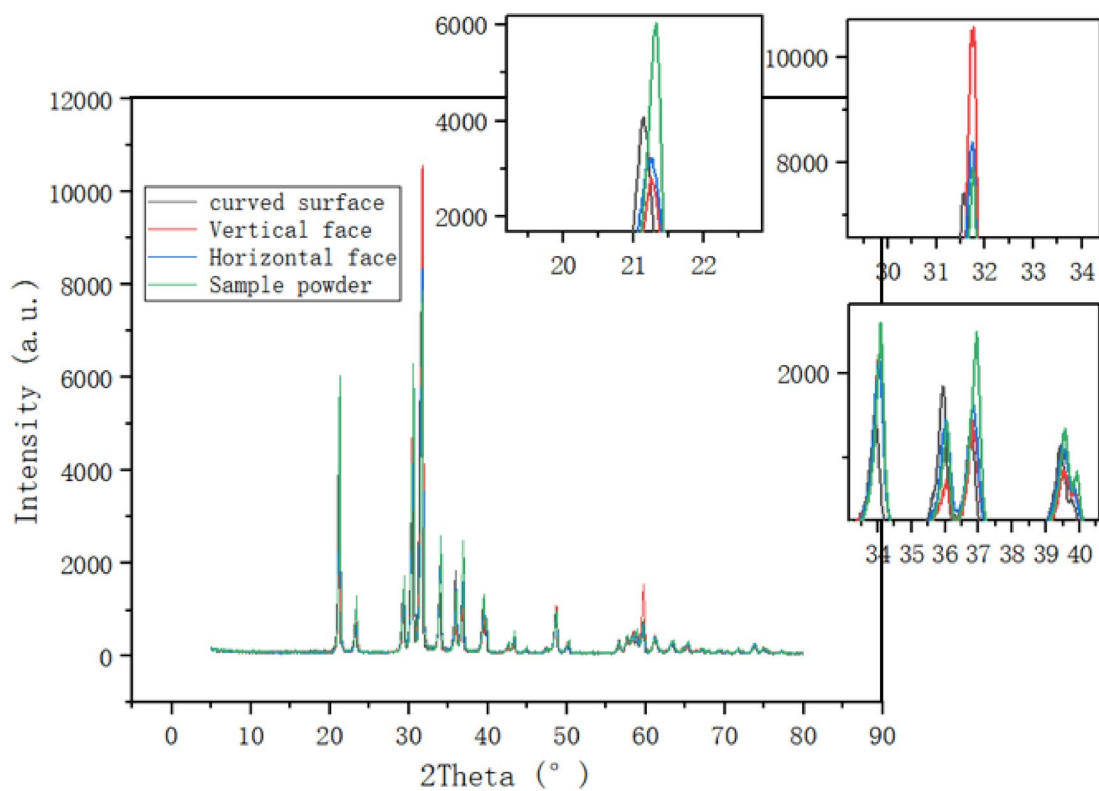


**Fig. 15.** XRD analysis charts.

The abscissa in the figure is twice the angle of incidence of the X-ray; Scan samples from  $5^\circ$  to  $80^\circ$  at a scan rate of  $8^\circ/\text{min}$ ; It can be seen from the Fig. 15 that the peak values appear between  $\theta = 15^\circ \sim 16.5^\circ$ ; Among them, the ordinate of the horizontal plane is shifted upwards by 8,000 units, and the ordinate of the vertical plane is shifted upwards by 16,000 units. From the Fig. 15: The peak value of the vertical plane is  $10000\text{a.u.} \sim 11000\text{a.u.}$ ; The peak of the horizontal and curved planes is  $7500\text{a.u.} \sim 8000\text{a.u.}$

XRD analysis revealed that all four materials exhibited diffraction peaks reaching maximum intensity at approximately  $2\theta = 31.5^\circ \sim 32^\circ$ . Notably, the vertical plane demonstrated the highest diffraction peak intensity, indicating both greater crystalline phase content and larger grain size in this orientation. Conversely, the horizontal plane showed the lowest peak intensity, suggesting reduced crystallinity and smaller grain dimensions. These findings are consistent with experimental observations where vertical surfaces facilitated more abundant crystal growth while horizontal surfaces presented the greatest crystallization challenges, resulting in sparser crystal formation.

## Conclusions

This research found that the grain size of lithium carbonate under microscopic examination is mainly related to the container, temperature, evaporation rate, and growth direction.

Based on the above experiments, summary regarding the crystallization characteristics of lithium carbonate: selecting materials containing oxygen or with good hydrophilicity as crystallization substrates and using fine hair strands as an induction medium to achieve the transformation of lithium carbonate from powder to crystals. At the same time, the size of the crystals can be adjusted by controlling the evaporation rate and environmental temperature. Then select the vertical plane or curved surface to determine the growth direction of the crystal.

Regarding the research results, it can be conclude that using a glass beaker (GG-17) as the carrier, selecting the curved surface as the growth direction, covering the glass beaker mouth with plastic film pore about 2 mm approximately, and controlling the temperature within the range of  $0^\circ\text{C}$  to  $10^\circ\text{C}$ , the crystal growth is optimal (large volume and regular morphology). Compared with the volume of lithium carbonate crystals obtained in previous studies, there is a significant increase.

In the following experiment, multiple strands of hair twisted into ropes will be used and immersed in a lithium carbonate solution to achieve lithium extraction.

## Data availability

Data available on request from the author: Cheng-Lu Jiang, email: [juul@sicau.edu.cn](mailto:juul@sicau.edu.cn).

Received: 3 June 2025; Accepted: 30 September 2025

Published online: 06 November 2025

## References

1. Peng, J. Analysis of domestic lithium carbonate production process and benefits salt. *Sci. Chem. Eng.* **48** (10), 18–21 (2019).
2. Wenfeng, M., Lu, W., Li, J., Sun, J. & Chen, M. Preparation of  $\text{Li}_2\text{CO}_3$  powder nanoparticles by vacuum freeze drying. *Ceram. Int.* **47** (22), 32237–32242 (2021).
3. Yao, Y. et al. Hydrometallurgical processes for recycling spent Lithium-Ion batteries: A critical review. *ACS Sustain. Chem. Eng.* **6** (11), 13611–13627 (2018).
4. Huo, H. et al.  $\text{Li}_2\text{CO}_3$ : A critical issue for developing solid Garnet batteries. *ACS Energy Lett.* **5** (1), 252–262 (2020).
5. Yang, J., Yu, Y., Yu, J. & Wang, X. Development trend and countermeasures of China's lithium energy storage industry energy conservation in nonferrous metallurgy. *38* (02), 28–30. (2022).
6. Jiang, S., Ma, L., Jiang, G., Wen, H. & Jiang, X. Analysis of transient heat generation characteristics during the discharge process of lithium-ion batteries. *J. Power Sources.* **17** (02), 171–177 (2019).
7. Huang, H., Jia, X., Cheng, K. & Xu, J. Adequacy assessment and guarantee mechanism of multi-resource power generation capacity under the new power system automation of the power system. 1–14.
8. Zhang, Y. Preliminary thinking on building a new energy system to achieve the double carbon goal petroleum science and technology forum. 1–10.
9. Ma, J. et al. Development status and countermeasures of Lithium-ion battery energy storage industry Zhejiang chemical industry. *53* (12), 17–23. (2022).
10. Qi, Z. et al. Research progress on industrialization technology of lithium extraction from Brine in salt lake in China inorganic chemicals industry. *54* (10), 1–12. (2022).
11. Tao, Z. Research on the preparation of battery-grade lithium carbonate from salt lake lithium carbonate. 3 (2016).
12. Xu, X. The 2023 National High-level forum on lithium extraction and Brine resources development in salt lakes was successfully held water treatment technology. *49* (04), 66. (2023).
13. Ma, G. et al. Research process on novel electrolyte of lithium-ion battery based on lithium salts. *J. Inorg. Mater.* **33** (7), 699–710 (2018).
14. Wang, Y. et al. Particle size and morphology control of lithium carbonate prepared by reaction crystallization. *Inorg. Chemicals Ind.* **48** (09), 13–17 (2016).
15. Zhang, C. & Zhao, Q. Preparation process of spherical fine lithium carbonate powder. *J. Southwest. Univ. Nationalities (Natural Sci. Edition)* (02), 326–329. (2008).
16. Duan, S., Sun, Y., Song, X. & Yu, J. Response surface method to optimize the reaction crystallization process of lithium carbonate. *CIESC J.* **68** (11), 4169–4177 (2017).
17. Liang, Y. & Fan, L. Mechanical failures in solid-state lithium batteries and their solution. *Acta Phys. Sinica.* **69**, 22 (2020).
18. Zhang, A., Wang, C., Zhao, S., Chang, Z. & Wang, J. Research progress on Cathode/Electrolyte interface properties in Solid-State. *Batteries Mater. Eng.* **50** (11), 46–62 (2022).
19. Xie, J., Huang, L., Zhang, W., Xiong, T. & Wang, B. Effect of dispersion on the accuracy of laser particle size analyzer in detecting lithium carbonate particle size. *Distribution Shandong Industrial Technol.* (01), 122–127. (2024).
20. He, M., Chen, J., Hou, D. & Chen, Y. Fiber crystallizer: disruptive breakthrough in lithium extraction technology. *J. Salt Lake Res.* **31** (04), 1–2. (2023).
21. Sun, Y. Study on the crystallization process of lithium carbonate. 1–2 (2010).
22. Wang, B. Process study on crystallization optimization and morphology control of lithium carbonate reaction. (2021).
23. Nan, J., Wang, J., Wu, J. & Liu, J. Lithium immersion crystallization method for preparing snowflake-like single crystal high-purity lithium carbonate. 13 .
24. Dibyajyoti, K., Purabi, G. & Pankaj, D. Effect of ZnS nanoparticles on the spectroscopic transitions of  $\text{Ho}^{3+}$  ions in sol-gel silica matrix. *Ceram. Int.* **49** (17PA), 28392–28404 (2023).
25. Song, T., Pan, X., Zhao, Y. & Xia, W. Preparation of  $\text{Eu}^{2+}$  and  $\text{Dy}^{3+}$  co-doped  $\text{Sr}_2\text{MgSi}_2\text{O}_7$  translucent long afterglow glass-ceramics by recrystallization-melting and their luminescence properties. *Ceram. Int.* **50** (13 PB), 24864–24871 (2024).

## Author contributions

Yang Zhang: Investigation, Conceptualization, Methodology, Writing—Original draft preparation. Yu-Han Huang, Hou-Jie Wang, Lin-Guo Zheng, Qi-Yu Yang, Yan-Ru Wang: Investigation, Conceptualization, Methodology, Jiang Zhao: Investigation, Conceptualization, Resources, Cheng-Lu Jiang: Methodology, Writing—Reviewing and Editing.

## Declarations

### Competing interests

The authors declare no competing interests.

### Additional information

**Correspondence** and requests for materials should be addressed to C.-L.J.

**Reprints and permissions information** is available at [www.nature.com/reprints](http://www.nature.com/reprints).

**Publisher's note** Springer Nature remains neutral with regard to jurisdictional claims in published maps and institutional affiliations.

**Open Access** This article is licensed under a Creative Commons Attribution-NonCommercial-NoDerivatives 4.0 International License, which permits any non-commercial use, sharing, distribution and reproduction in any medium or format, as long as you give appropriate credit to the original author(s) and the source, provide a link to the Creative Commons licence, and indicate if you modified the licensed material. You do not have permission under this licence to share adapted material derived from this article or parts of it. The images or other third party material in this article are included in the article's Creative Commons licence, unless indicated otherwise in a credit line to the material. If material is not included in the article's Creative Commons licence and your intended use is not permitted by statutory regulation or exceeds the permitted use, you will need to obtain permission directly from the copyright holder. To view a copy of this licence, visit <http://creativecommons.org/licenses/by-nc-nd/4.0/>.

© The Author(s) 2025